COMPDYN 2013
4th ECCOMAS Thematic Conference on
Computational Methods in Structural Dynamics and Earthquake Engineering
M. Papadrakakis, V. Papadopoulos, V. Plevris (eds.)
Kos Island, Greece, 12–14 June 2013

EFFECT OF COUPLING EXCESS PORE PRESSURE AND SOIL DEFORMATION ON THE NONLINEAR RESPONSE

Silvana Montoya-Noguera[1] **and Fernando Lopez-Caballero**[1]

[1]Ecole Centrale Paris
Grande Voie des Vignes, F-92295 Chtenay-Malabry
{silvana.montoya-noguera},
{fernando.lopez-caballero}@ecp.fr

Keywords: Earthquake engineering, Site response, Soil nonlinearity, Liquefaction.

Abstract. *The development of excess pore pressure (Δp_w) and consequent reduction in effective stress leads to the softening of a liquefiable soil deposit that can alter ground motions in terms of amplitude, frequency content, and duration. To assess these effects in a 1D medium to loose sand model, two analysis were made: (1) A BIOT hydraulic and mechanical computation of a saturated soil deposit and (2) a mechanical computation of a dry soil with equivalent behavior. The results regarding the profile of maximum accelerations and shear strains, the surface accelerations and their corresponding response spectra ratio are analyzed. The mean values of the normalized response spectra ratio between the wet and dry surface acceleration show a deamplification of high frequencies (i.e. $f > 1.0Hz$) and an amplification of low ones that tend to increase with the liquefaction zone size. Coupling of Δp_w and soil deformation is therefore of great importance to accurately model the ground motion response. On the contrary, while peak acceleration predictions could be conservative, the amplification on the low frequencies could be largely underestimated which would be highly prejudicial for tall buildings.*

1 INTRODUCTION

The performance of structures during earthquakes is strongly influenced by the soils that support them. Local site effects can influence structures performance in two primary ways: by imposing additional deformations on the structure through ground failure and by influencing the ground motions that excite the structure. The reliable and economical seismic design of structures requires that local site effects on the ground motions be accurately predicted.

Usually, equivalent-linear models like the one employed in SHAKE [1] program are used to quantify the effect of soil deposits on propagated ground motions. Moreover and in most cases, effects of local soil deposits are only included as an attenuation of the maximum acceleration at surface [2]. However, the behavior of liquefiable soils is dominated by pore pressure generation which is not included in these models. This paper studies numerically the effect of excess pore pressure (Δp_w) on the nonlinear response of liquefiable soils. For this purpose an elastoplastic multi-mechanism model, known as ECP model [3, 4], is used to represent the soil behavior. The soil deposit was subjected to 78 unscaled earthquake signals chosen from the Pacific Earthquake Engineering Research (PEER) Center database.

First of all, nonlinearity induced by both strong ground motion and liquefaction apparition was studied via a 1-D numerical modelling of a saturated sand deposit. Then and in order to solely quantify the effect of Δp_w on the nonlinear response of the sand deposit, two mechanically-equivalent models -one saturated and one completely dry - were analyzed. Three aspects of the motion response are evaluated: i) the maximum acceleration and shear strain profile, ii) the maximum surface acceleration and iii) the corresponding acceleration response spectra.

2 NUMERICAL MODEL

2.1 Model description

The studied site is composed principally of 20m of medium to loose sand with an average shear wave velocity ($V_{s,\,20}$) close to 200 m/s, corresponding to ground type C of Eurocode 8 [5]. As shown in figure 2a, the shear modulus of the soil increases with depth. The characteristic elastic site period (T_s) of the soil is calculated by a transfer function between the Fourier transforms of accelerations in the surface and at the bottom of the soil deposit, for a sample signal at very low amplitudes (e.g. $PHA \approx 1E-5g$) to ensure elastic soil behavior. The first amplification peak corresponds to the T_s and is approximated to 0.27s (see figure 2b). The saturated soil has a ground water table placed 1 meter below the surface and an impervious deformable bedrock is placed at the bottom of the column. The bedrock is assumed to follow an isotropic linear elastic behavior with a V_s equal to 551m/s.

2.2 Finite element mesh

As the soil is assumed to be horizontally homogeneous, 1D $u-p_w$ coupled finite element computations with plain-strain assumption were performed. The general purpose finite element code GEFDyn [6] was used . The saturated soil was modelled using quadrilateral isoparametric elements with eight nodes for both solid displacements and fluid pressures. The thickness of the elements is 0.5m, which is in agreement with the suggestions made by Foerster and Modaressi [7] to prevent numerical dispersion. An implicit Newmark numerical integration scheme is used in the dynamic analysis. The numerical parameters were calculated by the methodology of Kontoe et al. [8], by which γ and β are calculated from the spectral radius at infinity ρ_∞ to

achieve an "optimal high-frequency dissipation with minimal low-frequency impact". Furthermore, in order to quantify the numerical damping ξ related to these parameters a calibration procedure [9] was performed. Thus, a ρ_∞ equal to 0.8 is used, which corresponds to γ=0.611, β=0.301 and ξ equal to 1.64%.

Concerning boundary conditions and as the response of an infinite semi-space is modelled, equivalent boundaries have been imposed on the nodes of lateral boundaries (i.e. the normal stress on these boundaries remains constant and the displacements of nodes at the same depth in two opposite lateral boundaries are the same in all directions) [10]. For the bedrocks boundary condition, paraxial elements simulating deformable unbounded elastic bedrock have been used [11]. The vertically incident shear waves, defined at the outcropping bedrock, are introduced into the base of the model after deconvolution. Thus, the obtained movement at the bedrock is composed of the incident waves and the reflected signal.

2.3 Input earthquake motion

In order to define appropriate input motions to the non-linear dynamical analysis, a selection of recorded accelerograms are used. The adopted earthquake signals are proposed by Bradley et al. [12] and Sorrentino et al. [13]. Thus, 78 unscaled records were chosen from the Pacific Earthquake Engineering Research Center (PEER) database. The events range between 5.8 and 7.7 in magnitude and the recordings have site-to-source distance from 10 to 150km and dense-to-firm soil conditions (i.e. 30m averaged shear-wave velocity ($V_{s\,30}$) between 270 and 800m/s).

The statistics of some earthquake parameters calculated at outcropping conditions are shown in table 1. These intensity measures are peak horizontal acceleration (PHA), peak ground velocity (PGV), mean period (T_m), predominant period (T_p), period of equivalent harmonic wave ($T_{V/A}$), Arias intensity (I_a), significant duration ($t_{5\,95}$), root-mean-square intensity (I_{rms}), spectral intensity (SI) and specific energy density (SED). The coefficient of variation (CV) is above 50% for almost all parameters and it is above 100% for I_a. A higher variation in I_a is of great importance given that after the sensitivity analysis performed by Lopez-Caballero and Modaressi-Farahmand-Razavi [14], it was proved to be the most influential input variable on the liquefaction index ($Q_{H=10}$). Figure 1 shows the response spectra of all the input earthquake motions; accelerations were filtered to 15Hz and the spectral amplitude has a 5% structural damping. Similarly, a great variation is presented on the response spectra.

Table 1: Earthquake characteristics

Parameter	Range	Mean	CV [%]	Median
PHA [g]	0,05 - 0,91	0,25	65	0,18
PGV [cm/s]	4,82 - 69,95	23,44	62	21,08
T_m [s]	0,22 - 1,02	0,61	32	0,58
T_p [s]	0,08 - 1,38	0,4	66	0,35
T_{VA} [s]	0,21 - 2,43	0,53	64	0,45
I_a [m/s]	0,04 - 3,16	0,74	102	0,41
$t_{5\,95}$ [s]	2,92 - 62,13	15,84	76	11,7
I_{rms} $[m/s^2]$	0,07 - 0,88	0,29	63	0,23
SI [m]	0,21 - 2,55	0,85	59	0,77
SED $[cm^2/s]$	34,51 - 11646	1098,5	184	497,86

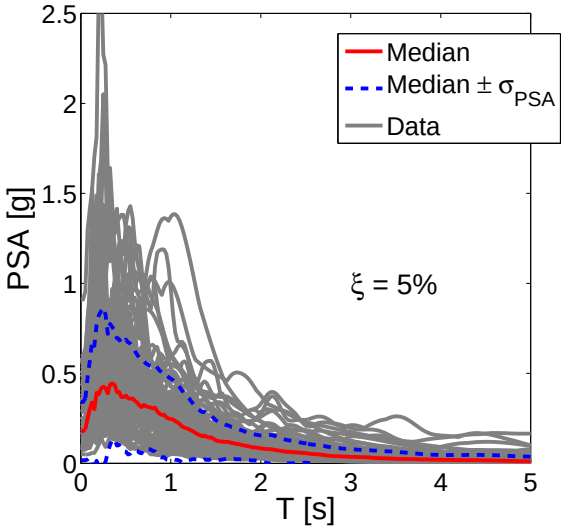

Figure 1: Response spectra of earthquake motions

2.4 Soil constitutive model

The soil behavior is simulated with the elastoplastic multimechanism model developed at Ecole Centrale Paris, ECP model also known as Hujeux model. This model can take into account the soil behavior in a large range of deformations. The model is written in terms of effective stresses. The model uses a Coulomb type failure criterion and the critical state concept. The evolution of hardening is based on the plastic strain (deviatoric and volumetric strains for the deviatoric mechanisms and only volumetric strain for the isotropic one). To take into account the cyclic behavior it uses a kinematical hardening which relies on the state variables at the last load reversal. The soil behavior is decomposed into pseudo-elastic, hysteretic and mobilized domains. Refer to Aubry et al. [3], Hujeux [4], Lopez-Caballero and Modaressi-Farahmand-Razavi [14] among others for a complete understanding of the ECP model. The soil parameters were determined with the procedure defined in Lopez-Caballero et al. [15] and are shown in table 2. The verification of these parameters and some laboratory test simulations can be found in Lopez-Caballero and Modaressi-Farahmand-Razavi [14].

3 EFFECT OF INDUCED PORE WATER PRESSURE

In order to solely quantify the effect of induced pore water pressure (Δp_w) on the nonlinear response of the sand deposit, two mechanically-equivalent models -one saturated and one completely dry - were analyzed. Firstly, to ensure that the only difference in these models behavior is due to pore water pressure generation, the shear modulus profile and transfer function are evaluated. The obtained maximum shear modulus profiles are shown in figure 2a for the elastic behavior and except for some differences at G_{max} at the bottom of the column, the initial behavior of both soils is identical. Therefore, it is proved that differences in the response will be due only to the effect of Δp_w on the wet column.

The spectral ratio, shown in figure 2b is the ratio between the Fourier transform of the motions at the ground surface and the bedrock. It characterizes the amplification produced by the soil deposits [9]. Both models present the same predominant frequencies (also called characteristic frequencies), although the dry column present lower amplifications.

Table 2: ECP model's parameters for the soil column

rho_s (kg/m^3)	2700
n $(\cdot)$	0.47
Elasticity	
K_{ref} (MPa)	628
G_{ref} (MPa)	290
n_e	0.5
p_{ref} (MPa)	1.0
Critical State and Plasticity	
ϕ'_{pp} $(\cdot)$	30
β	33
d	2.0
b	0.2
p_{co}(kPa)	81.80
Flow Rule and Isotropic Hardening	
$\psi'(\cdot)$	30
α_ψ	1.0
a_1	1.0E-4
a_2	2.0E-3
c_1	2.0E-3
c_2	1.0E-3
m	1.5
Threshold Domains	
γ^{ela}	5.0E-3
γ^{hys}	4.0E-2
γ^{mob}	8.0E-1
γ^{ela}_{iso}	1.0E-3

3.1 Peak surface acceleration

Regarding the relation between the peak horizontal acceleration at outcropping (PHA) and received at the surface (PGA), figure 3a shows an amplification of the signal for PHA less than 0.2g. As shown by others [16, 14, 17], in this case it appears that this value is a threshold for nonlinearity due to the ground motion. Above this threshold, the peak acceleration at surface is bigger for the dry column as the attenuation given by the liquefaction apparition is not present. Nonetheless, it appears some attenuation probably caused by the soil resistance degradation.

Figure 3b expresses the peak surface accelerations (PGA) of the dry column as a function of PGA of the wet column ranged by the Liquefaction Index (Q) for a selected depth H. This value is defined by Shinozuka and Ohtomo [18] as:

$$Q_H = \frac{1}{H}\int_0^H \frac{\Delta p_{w\,end}(z)}{\sigma'_{v0}(z)}\mathrm{d}z \tag{1}$$

where $\Delta p_{w\,end}$ is the difference between the pore water pressure at the begging and at the end of the input motion at a certain depth z and σ'_{v0} is the initial effective vertical stress at the same depth. The Q value indicates the ratio of liquefaction initiation for a selected depth at the end of shaking. A value of 1.0 indicates conditions of initial liquefaction throughout the H meters column. As shown in the figure 3b, PGA values for the dry column can be twice as big as the

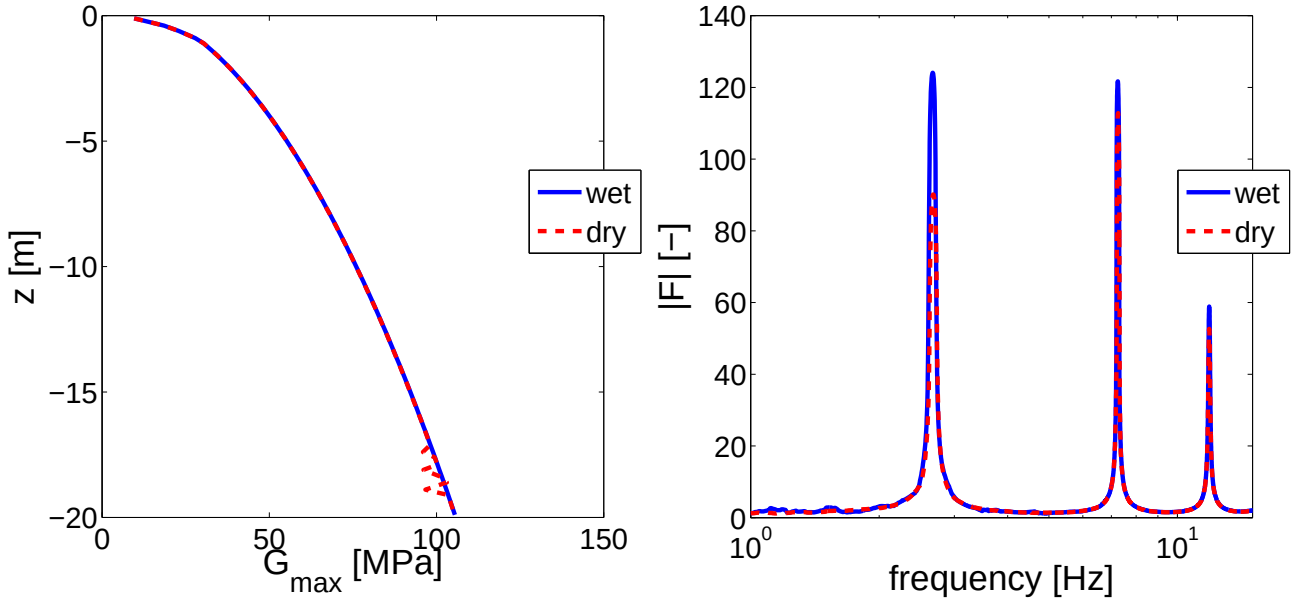

(a) (b)

Figure 2: Elastic behavior a) G_{max} profile and b) transfer function

ones of the wet column; moreover it appears to be a relationship between these differences and the liquefaction index Q.

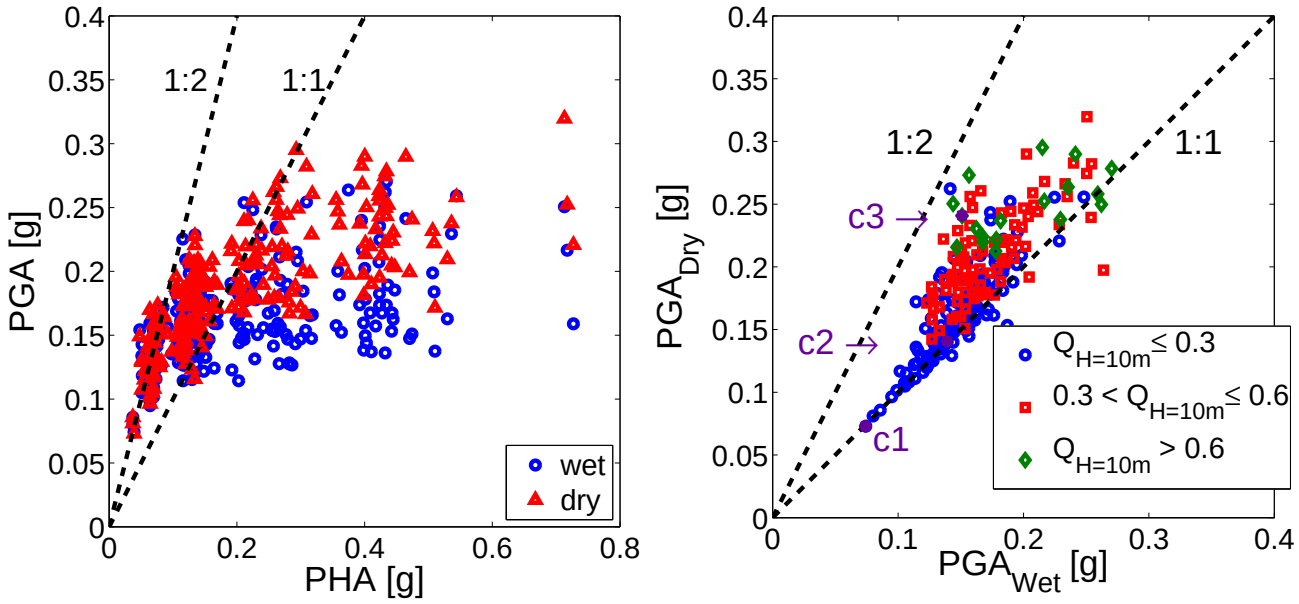

(a) (b)

Figure 3: a) Peak ground acceleration at free field (PGA) as a function of peak horizontal acceleration at outcropping (PHA) and b) PGA of the dry and wet column grouped by Liquefaction index

3.2 Acceleration profile

For the purpose of analyzing the motion variation throughout the soil deposit, three cases were studied: c1) $PHA \simeq 0.05$g, c2) $PHA \simeq 0.15$g and c3) $PHA \simeq 0.5$g (shown in figure 3b). For the first case, both columns amplify the maximum acceleration by a factor of 2; for the second one, PGA is almost equal to PHA; and for the last case, the peak acceleration is greatly attenuated (i.e. $PGA \simeq 0.5PHA$). Moreover, the difference between dry and wet columns increases with cases. The time history profiles of the pore pressure ratio ($r_u(t) = \Delta p_w(t)/\sigma'_{v0}$) are shown in figure 4. The darkest blue color is $r_u = 0$ and the darkest red one is $r_u = 1.0$. Case 1 is not shown as r_u is less than 0.2 throughout the profile, while for the second case, starting at 7s, between 6 and 15m depth r_u values are greater than 0.5 and by 7m there is a concentrated totally liquefied zone (i.e. $r_u = 1.0$) from about 10s until the end of shaking. Case 3, however, presents two strong liquefied zones at around 2 to 5m and between 8 and 10m; the first one starting at 3s and the deeper one at 5s. Concerning the time history, it appears to be two clear drops of pore pressure at 5s and 8s, with others smaller ones in between. Finally, after 12s, pore pressure starts to gradually increase and spread through the soil deposit. It is interesting to note that while the same soil is tested, different motions liquefy different depths.

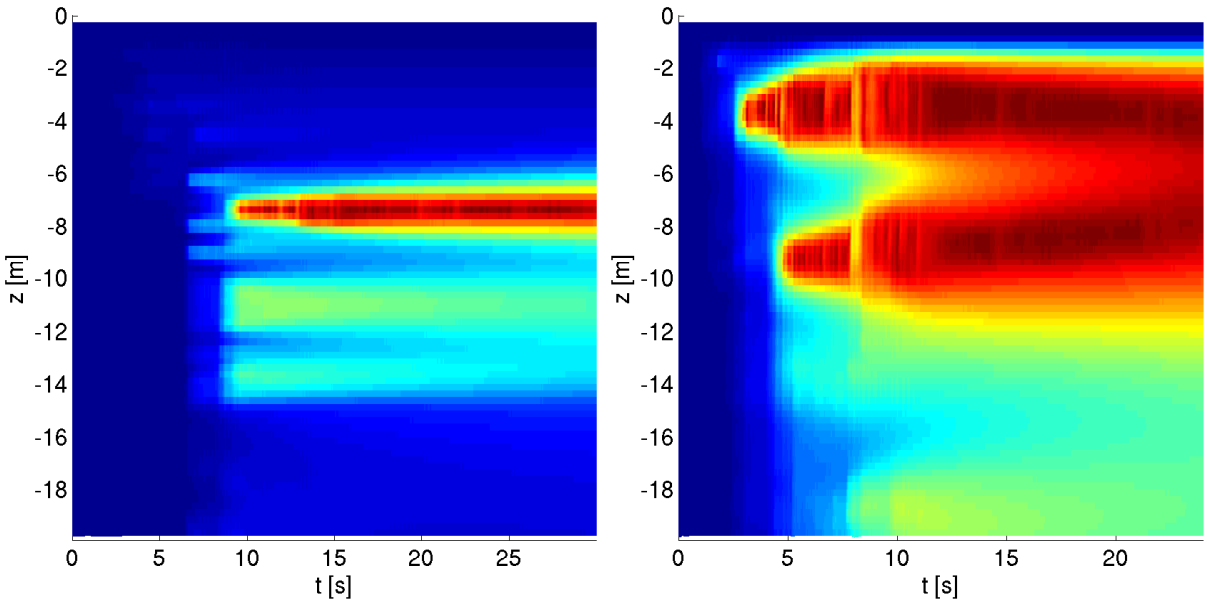

Figure 4: Time history of r_u profile a) c2 point and b) c3 point

In figure 5 the profiles of the pore pressure ratio r_u at the end of shaking, the maximum acceleration and the maximum absolute shear strain (γ) are shown for the three cases. In the first case, in figure 5a, it is clear that the peaks on the acceleration profile correspond to the peaks on shear strain at about 6 to 8m, whereas peaks on r_u are some meters above. As for the dry column, there are no relevant peaks neither on the acceleration nor the γ profile. Rather small differences on the PGA between the wet and dry column can be due to the low pore pressure ratio presented along the profile ($r_{u\,end} < 0.1$). As for the second case, in figure 5b, liquefaction initiated around 8m (i.e. $r_{u\,end} > 0.8$). The a_{max} profile presents almost the same peak with a maximum three times bigger than PHA value at 8m. The γ profile also presents it maximum

at the same depth, although other spikes are presented. By the other hand, the dry column presents some differences between the maximum on acceleration and on shear strain, which are presented some meters below. Finally, for the third case shown in figure 5c, liquefaction is presented from 3 to 10m, which as seen in figure 3a, gives to an attenuation of the PHA value in the wet column. In it, although the a_{max} profile is decreasing as it climbs up to the surface, four spikes can be distinguished at around 2, 5, 10 and 15m. These are also present at the $|\gamma_{max}|$ profile, with strains 6 times bigger than the average. Regarding the dry column, and like in the other cases, spikes in the a_{max} and $|\gamma_{max}|$ profiles are much smaller and are not related to those of the wet column. On the whole, shear strains are always smaller for the dry column, i.e. without the effect of coupled excess pore water pressure with deformation.

3.3 Acceleration response spectra

The influence of coupling excess pore water pressure to deformations is asset by calculating the response spectra of the surface acceleration from the wet and dry column. Because of the variation of the frequency content and by means of arriving to a general conclusion, the acceleration-time histories are divided into three cases which are then studied separately. The input motion accelerogram and the pore pressure ratio at the end of shaking evaluated at 10m depth in the wet model are shown in figure 6 for the three cases. As in the previous figure, the spikes on acceleration correspond to the rapid increase of r_u (e.g. at 8s in figure 6c. Two vertical lines show the t_5 and t_{95} values, defined as the time where 5 and 95% of Arias intensity is reached, which roughly coincides with the start and end of the r_u increase. These lines will be used to separate the different time windows.

The response spectra at different time windows are plotted in figure 7 for the three cases and the three time windows. For the first case, $r_u(z = 10m) \leq 0.03$, the three time windows present near match between both columns which confirms that significant softening did not occur. While for the second and third cases, only for the first time window (i.e. prior to significant rise of pore pressure), responses of the wet and dry columns are similar. Afterwards and for short periods, the dry column produced a much higher peak whereas the coupling of excess pore pressure and its subsequent soil softening inhibits the transfer of the intense high-frequency peaks to the ground surface. For long periods, the wet column presents larger spectral values than the dry column. As the r_u value increases, i.e. in the third case (figure 7c), the difference between columns increases: for the wet column, amplification of long periods and for the dry one, amplification of short periods.

3.3.1 Normalized response spectral ratio

In order to assess the effect of the soil stiffening on the frequency content of the surface signal, Hartvigsen [19] proposed to characterize the effects of pore pressure with a response spectral ratio. Moreover, because the reduction in spectral acceleration showed for periods below about 1s is related to the differences between signals, the response has to be normalized. Therefore the normalized response spectral ratio (NRSR) is defined as:

$$NRSR(T) = \frac{PSA_{wet}(T)/PSA_{wet}(T=0)}{PSA_{dry}(T)/PSA_{dry}(T=0)} \tag{2}$$

where $PSA_{wet}(T)/PSA_{wet}(T=0)$ correspond to the normalized response spectrum at surface when saturated and $PSA_{dry}(T)/PSA_{dry}(T=0)$ is the normalized response spectrum when dry. The responses were divided in three groups according to the $Q_{H=10m}$ value obtained when

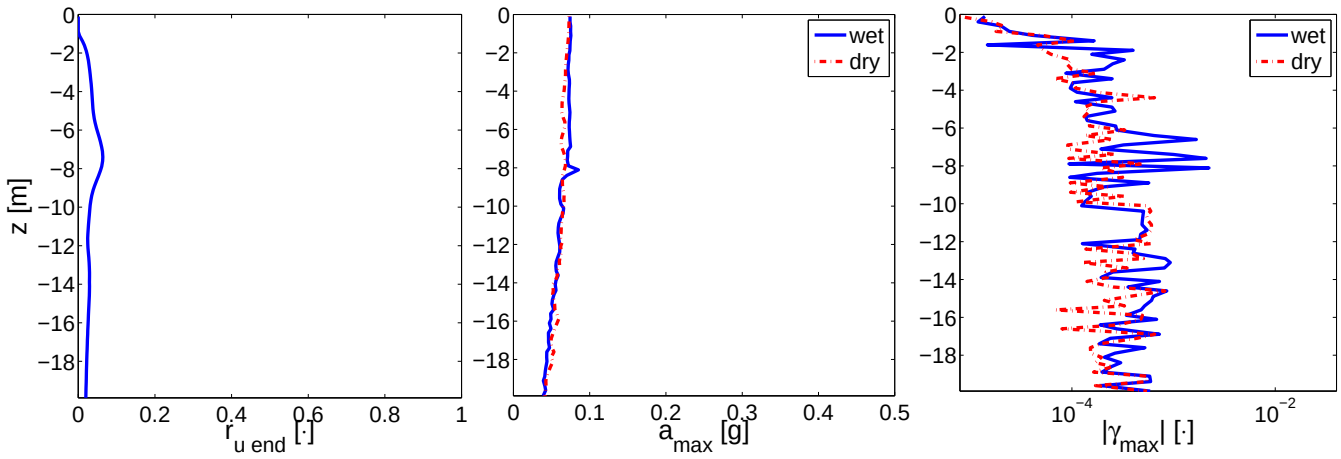

(a) case 1

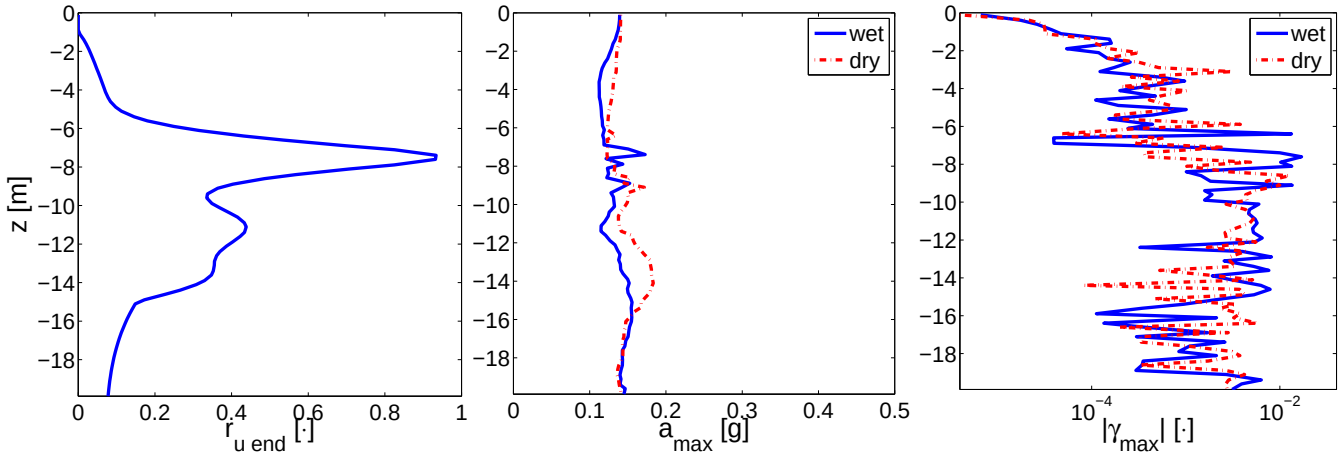

(b) case 2

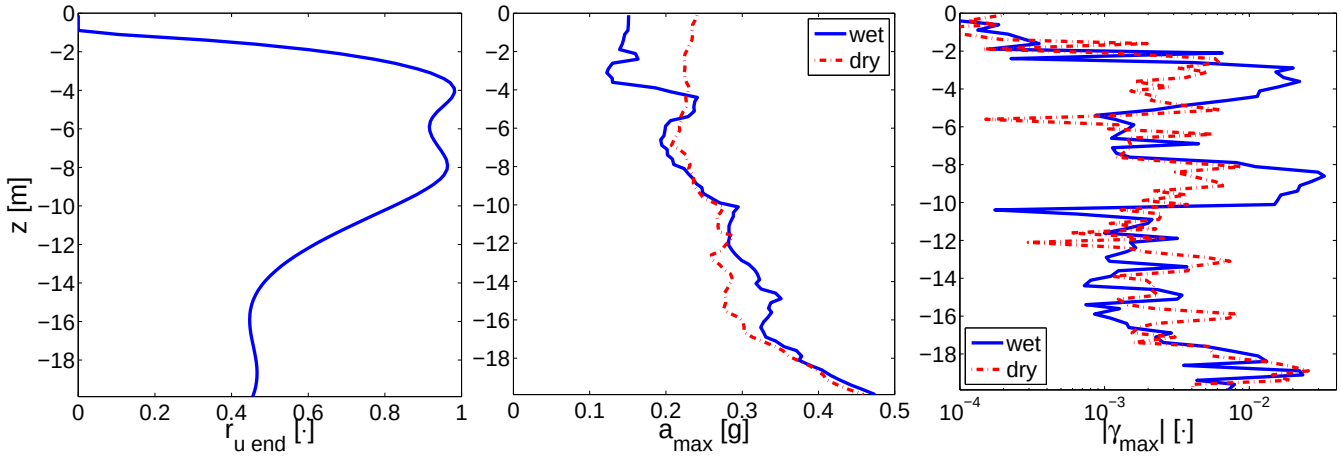

(c) case 3

Figure 5: Maximum r_u, acceleration and γ profile

saturated, namely, $Q_{H=10m} \leq 0.3$, $0.3 < Q_{H=10m} \leq 0.6$ and $Q_{H=10m} > 0.6$. Figure 8 displays the mean NRSR curves obtained for each time window. It is interesting to note how as the liquefaction potential increases, the NRSR increases for the high periods (i.e. $T > 1.0s$). As a result, high period amplification in the more liquefied soils is not considered in models that

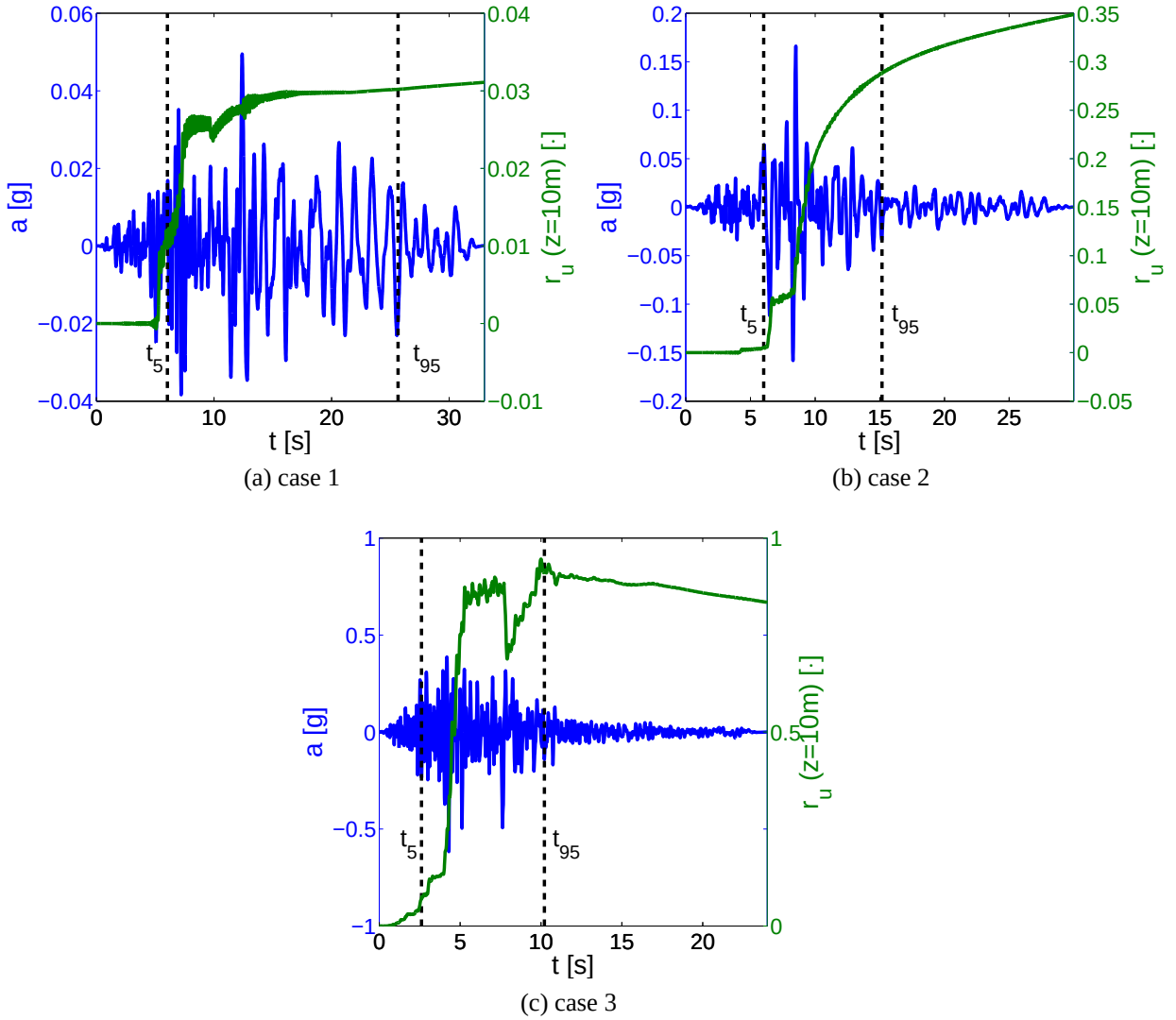

(a) case 1

(b) case 2

(c) case 3

Figure 6: Time history of input acceleration and r_u at 10m depth (wet model)

lack of coupling pore pressure and responses of buildings with high predominant periods could be unconservative.

As an attempt to include the effects of pore pressure generation, several authors [19, 20] have proposed functions relating the amplification of the acceleration with the seismic hazard and the soil properties. However, given the great variability of the spectral ratio with period, it is unlikely to capture the detailed effects of Δp_w coupling on individual response spectra with an overall function. As an example the variation in figure 8b is shown in figures 9. The NRSR of all simulations are presented together with the mean and median values. Results are divided for each liquefaction index level. Due to the proper input motion variability, individual cases can be somewhat different of the general case (e.g. $Q_{H=10m} \leq 0.3$ in figure 9a); although, with a greater amount of simulations a relation could be given from a probabilistic framework. Nonetheless, for a complete analysis of important structures the use of a constitutive model with coupling excess pore pressure and soil deformation is required.

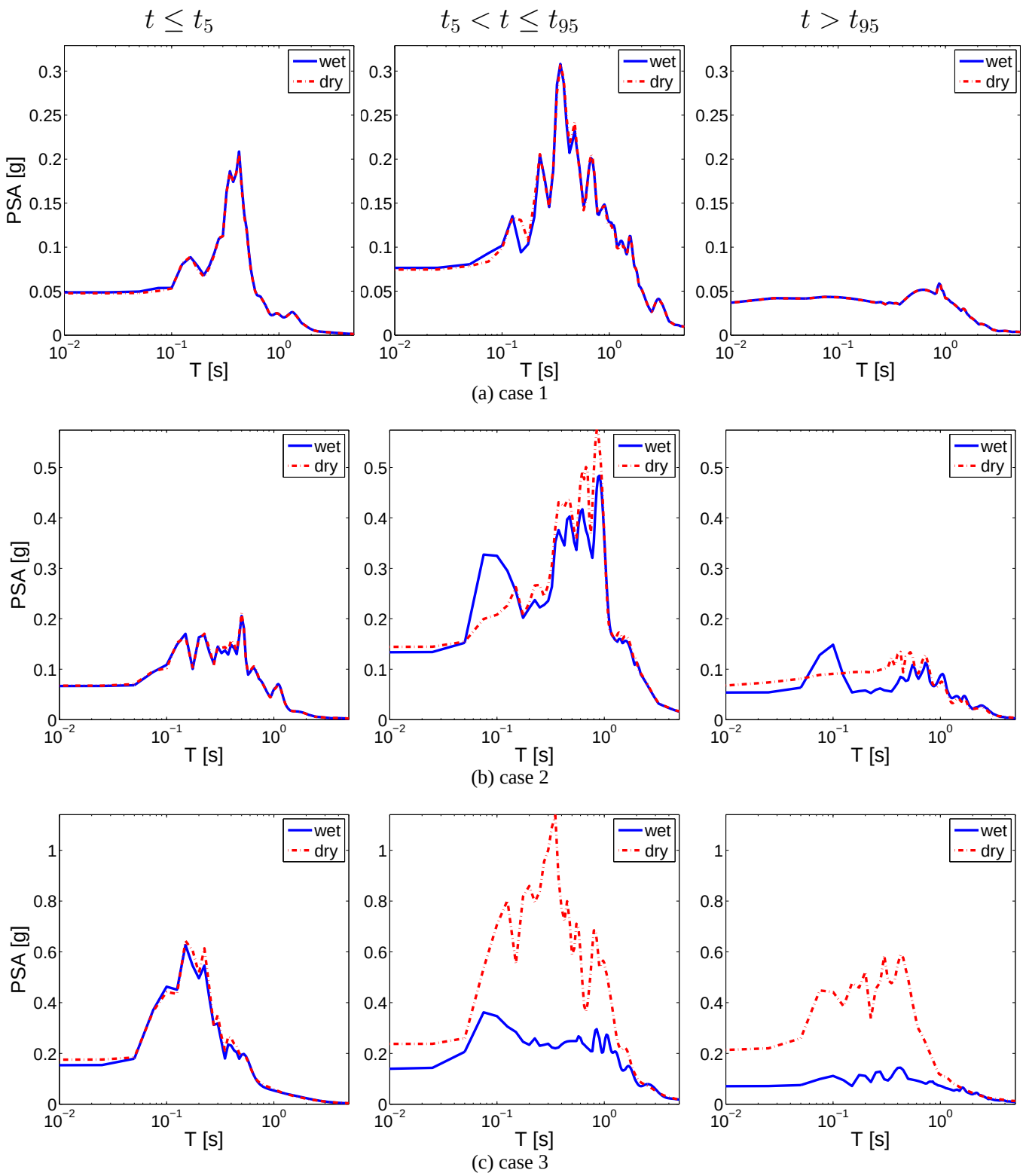

Figure 7: Response spectra at different time windows

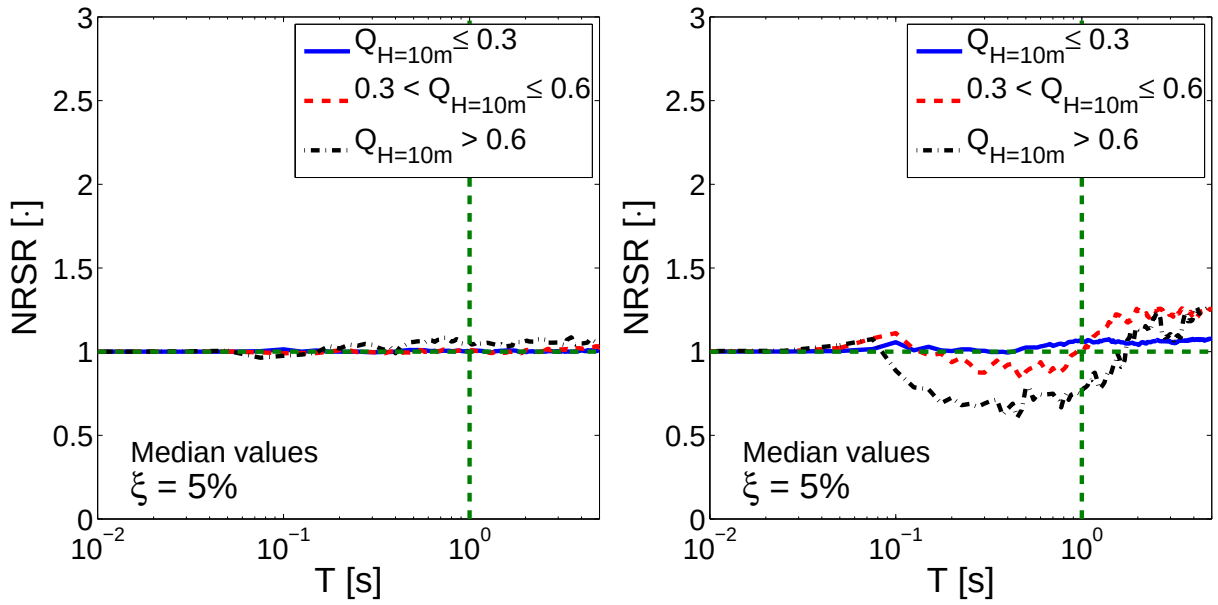

(a) $t \leq t_5$ (b) $t_5 < t \leq t_{95}$

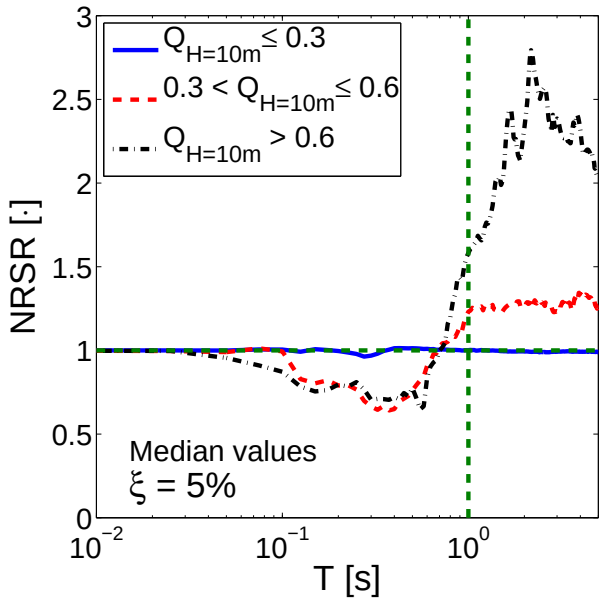

(c) $t > t_{95}$

Figure 8: Median Normalized Response Spectral Ratio NRSR values ranged by Q levels for each time window

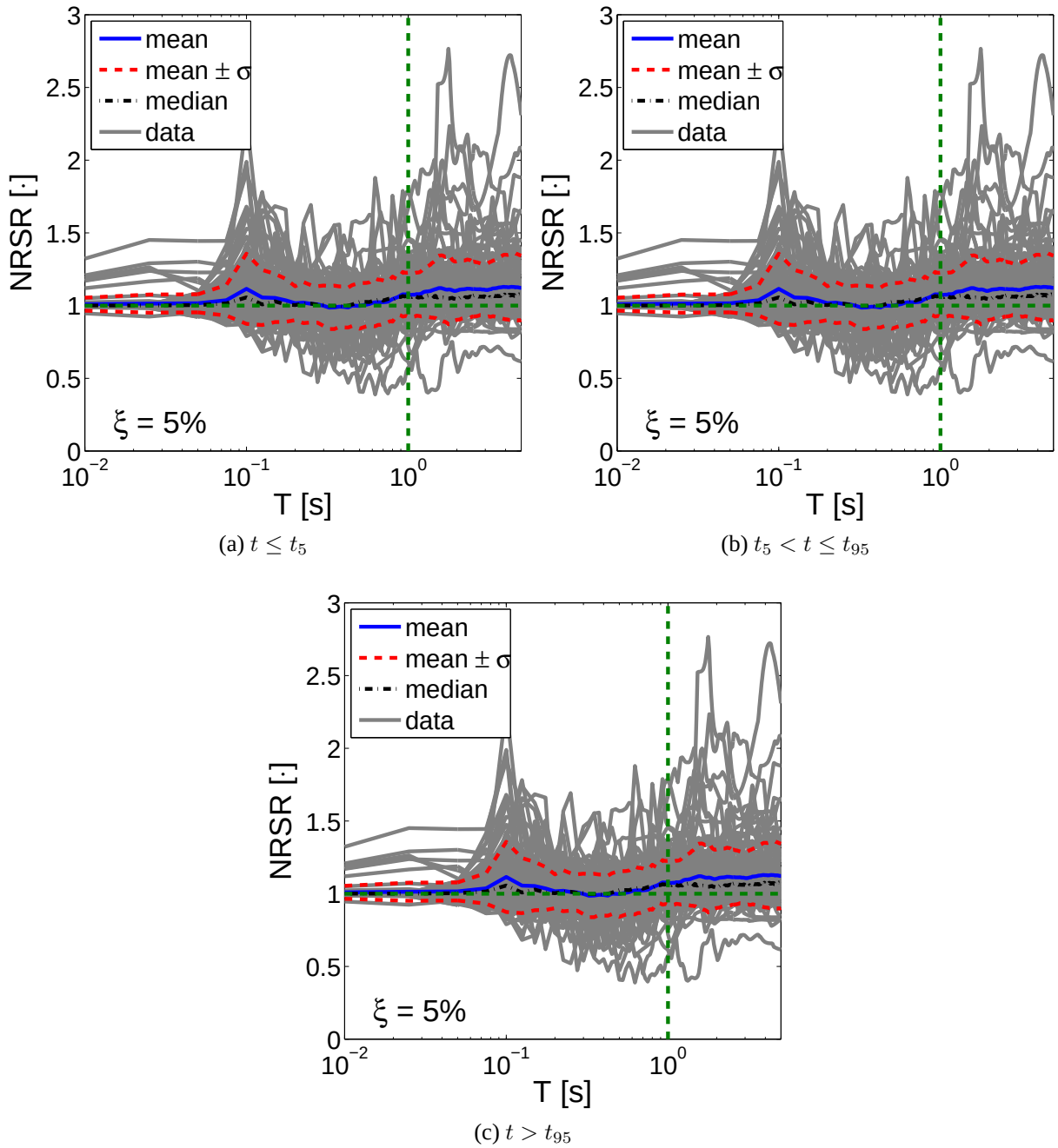

(a) $t \leq t_5$

(b) $t_5 < t \leq t_{95}$

(c) $t > t_{95}$

Figure 9: Median Normalized Response Spectral Ratio NRSR values ranged by Q levels for each time window

4 CONCLUSIONS

A finite element analysis was used to investigate the effect of coupling excess pore pressure and soil deformation on the nonlinear response. A typically liquefiable soil profile of 20m has been used. Two mechanically equivalent models were subjected to 78 unscaled earthquake motions: one taking into account coupling (wet column) and one without (dry column). The main conclusions drawn from this study are as follows:

- The acceleration is amplified at surface for small input motions (i.e. $PHA \leq 0.2$g) in the dry as well as in the wet column. Nonetheless, deamplification for strong ground motions is more significant in the wet column and it increases with PHA. As a result, models that do not include coupling of excess pore pressure will predict bigger surface accelerations.

- It appears that the difference between maximum surface acceleration for the two columns is directly related to the Liquefaction Index ($Q_{H=10}$), hence as the liquefaction zone increases the need for a more complete model is required.

- Regarding the soil behavior throughout the profile, it can be concluded that spikes of acceleration are found at the same depth than spikes of shear strain and maximums on liquefaction ratio for the wet column; however, shear strains spikes on the dry column do not correspond to spikes in acceleration and thus other mechanisms are involved.

- Concerning the response spectra, it appears that the dry column overestimate the amplification of low periods while it underestimates it for high periods. This variation is more important in the time period after the 95% of Arias intensity as the soil has softened on the wet column. Moreover, this variation increases with the liquefaction zone.

- From a probabilistic point of view, the response spectra follows the same trend; although the variation between one event and another is significant. Therefore a generalization would be unlikely to capture the detailed effects of pore pressure coupling.

References

[1] P.B. Schnabel, J. Lysmer, and H.B. Seed. Shake: A computer program for earthquake response analysis of horizontally layered sites. Report no. eerc 72-12, Earthquake Engineering Research Center, 1972.

[2] T. L. Youd and S. K. Noble. Magnitude scaling factors. Technical report, National Center for Earthquake Engineering Research, State University of New York at Buffalo, 1997.

[3] D. Aubry, J.-C. Hujeux, F. Lassoudire, and Y. Meimon. A double memory model with multiple mechanisms for cyclic soil behaviour. *Int. Symp. Num. Mod. Geomech*, pages 3–13, 1982.

[4] J.-C. Hujeux. *Génie Parasismique: Une loi de comportement pour le chargement cyclique des sols*, pages 278–302. Presses ENPC, France, v. davidovici edition, 1985.

[5] CEN European Committee for Standardization. *Eurocode 8: Design of structures for earthquake resistance*, 1998-1 part 1: general rules, seismic actions and rules for buildings. EN, Brussels, Belgium, 2004.

[6] D. Aubry and A. Modaressi. Gefdyn - manuel scientifique. *Ecole Centrale Paris*, 2005.

[7] E. Foerster and H. Modaressi. A diagonal consistent mass matrix for earthquake site response simulations. *4th International Conference on Earthquake Geotechnical Engineering*, June 2007.

[8] S. Kontoe, L. Zdravkovic, and D. Potts. An assessment of time integration schemes for dynamic geotechnical problems. *Computers and geotechnics*, 35:253–264, 2008.

[9] E. Saez. *Dynamic non-linear soil structure interaction*. PhD thesis, Ecole Centrale Paris, 2009.

[10] F. Lopez-Caballero and A. Modaressi. Numerical analysis: Specification and validation of used numerical methods. Fp7-sme-2010-1-262161, PREMISERI project, Paris, France, 2011.

[11] H. Modaressi and I. Benzenati. Paraxial approximation for poroelastic media. *Soil Dynamics and Earthquake Engineering*, 13(2):117–129, 1994.

[12] B. Bradley, R. Dhakal, G. MacRae, and M. Cubrinovski. Prediction of spatially distributed seismic demands in specific structures: Ground motion and structural response. *Earthquake Engineering and Structural Dynamics*, 39(5):501–520, 2010.

[13] L. Sorrentino, S. Kunnath, G. Monti, and G. Scalora. Seismically induced one-sided rocking response of unreinforced masonry faades. *Engineering Structures*, 30(8):2140–2153, 2008.

[14] F. Lopez-Caballero and A. Modaressi-Farahmand-Razavi. Assessment of variability and uncertainties effects on the seimic response of a liquefiable soil profile. *Soil Dynamics and Earthquake Engineering*, 30:600–613, 2010.

[15] F. Lopez-Caballero, A. Modaressi-Farahmand-Razavi, and Hormoz Modaressi. Nonlinear numerical method for earthquake site response analysis i- elastoplastic cyclic model and parameter identification strategy. *Bulletin of Earthquake Engineering*, 5(3):303–323, 2007.

[16] G. T. Zorapapel and M. Vucetic. The effects of seismic pore water pressure on ground surface motion. *Earthquake Spectra*, 10(2):403437, 1994.

[17] L. Bonilla, C. Gelis, and J. Regnier. The challenge of nonlinear site response: field data observations and numerical simulations. *Seismic Motion*, august 2011.

[18] M. Shinozuka and K. Ohtomo. *Proceedings of the second US-Japan workshop in liquefaction, large ground deformation and their effects on lifelines*, technical report Spatial severity of liquefaction, page 193206. NCEER, 1989.

[19] A. Hartvigsen. Influence of pore pressures in liquefiable soils on elastic response spectra. Master's thesis, University of Washington, 2007.

[20] P. Bazzurro and C.A. Cornell. Nonlinear soil-site effects in probabilistic seismic-hazard analysis. *Bulletin of the Seismological*, 94(6):2110–2123, 2004.